

# Performance Analysis for BICM Transmission over Gaussian Mixture Noise Fading Channels

Alireza Kenarsari-Anhari, *Student Member, IEEE*, and Lutz Lampe, *Senior Member, IEEE*

**Abstract**—Bit-interleaved coded modulation (BICM) has been adopted in many systems and standards for spectrally efficient coded transmission. The analytical evaluation of BICM performance parameters, in particular bit-error rate (BER), has received considerable attention in the recent past. In this paper, we derive BER approximations for BICM transmission over general fading channels impaired by Gaussian mixture noise (GMN). To this end, we build upon the saddlepoint approximation of the pairwise error probability (PEP) and a recently established approximation for the probability density function (PDF) of bit-wise reliability metrics for nonfading additive white Gaussian noise (AWGN) channels. We extend this PDF approximation to the case of GMN, and obtain closed-form expressions for its Laplace transform for fading GMN channels. The latter allows us to express the PEP and thus BER via the saddlepoint approximation. For the special case of fading AWGN channels the presented approximations are closed form, since the saddlepoint is well approximated by  $1/2$  for BICM decoding. Furthermore, we derive closed-form PEP expressions also for GMN channels in the high signal-to-noise ratio regime and establish the diversity and coding gain for BICM transmission over fading GMN channels. Selected numerical results for BER of convolutional coded BICM highlight the usefulness of the proposed approximations and the differences between AWGN and GMN channels.

**Index Terms**—Bit-interleaved coded modulation (BICM), performance analysis, Gaussian mixture noise, saddlepoint approximation, fading channels.

## I. INTRODUCTION

Bit-interleaved coded modulation (BICM) introduced in [1] and widely popularized through [2] has been adopted in many systems and standards for spectrally efficient coded transmission (see [3] for an up-to-date treatment of BICM). Alongside widespread adoption and deployment of BICM, its analysis has attracted considerable attention. In addition to the BICM union bound and expurgated bound approaches already presented in [2], a number of relatively recent works have been dedicated to arrive at semi-analytical bit-error rate (BER) approximations, cf. e.g. [4], [5], [6], [7], [8], [9]. Many of these build on the saddlepoint approximation (cf. [10], [11]), which was first proposed in [12] to analyze the performance of BICM. While this greatly simplifies the analysis, often numerical

integration is still required to compute the BER approximation [4], [12]. An analytical approach, based on the approximation of the probability density function (PDF) of reliability metrics (i.e., log-likelihood ratios (LLRs)), has been developed in [6], [7] for nonfading and Nakagami- $m$  fading channels with integer  $m$ , respectively, assuming square quadrature amplitude modulation (QAM) constellations with Gray labeling. Also for Nakagami- $m$  fading channels but taking into account the effect of finite interleaving, [8] derives BER approximations using a “large-SNR” analysis. Since this analysis considers a unique nearest-distance vector of competitive signal points, Gray labeling is required. Recently, in [9], we have developed an analytical approach for performance evaluation of BICM transmission over Nakagami- $m$  fading channels with general  $m$ . Our approach was based on an approximation of the PDF of LLRs which results in a mathematically tractable expression and thus allows further evaluation of performance parameters such as BER and cutoff rate using the saddlepoint approximation from [12].

While BICM has been thoroughly investigated for the additive white Gaussian noise (AWGN) case, the analysis of BICM transmission impaired by non-Gaussian noise has received relatively little attention, cf. e.g. [13], [14]. In general, the study of communication in non-Gaussian environments has become very popular due to its practical relevance. In many practical cases such as indoor radio communication, partial-time jamming, ultrawideband communication, and power line communication, this interference is well modeled as a Gaussian mixture noise (GMN) [15], [16], [17], [18], [19], [20], [21]. It is therefore of immediate interest to extend BICM performance analyses as those mentioned above to the case of GMN. To this end, the authors of [14] present a framework that modifies the BICM expurgated bound from [2] to encompass non-Gaussian noise. Since the analysis relies on the expurgated bound, it is limited to the case of Gray labeling and does not result in closed-form expressions for BER. Furthermore, the asymptotic performance analysis in [14] is valid only when the diversity order of the system is an integer.

In this paper, we present a novel approach for performance evaluation of BICM transmission over general frequency-flat fading channels impaired by GMN. As in [14] it is assumed that the system employs the standard Euclidean-distance decoder, which is an instance of mismatched decoding [22], [3], [23] in the presence of GMN. Our analysis mainly builds upon (i) the saddlepoint approximation proposed for BICM in [12] and (ii) the approximation of the PDF of bitwise reliability metrics from [9]. The main contributions of this work can be summarized as follows.

Manuscript received June 11, 2009; revised September 9 and December 9, 2009. This work was supported by the National Sciences and Engineering Research Council (NSERC) of Canada. The material in this paper was presented in part at the 2010 IEEE International Conference on Communications (ICC), Cape Town, South Africa, May 2010.

A. Kenarsari-Anhari was with the Department of Electrical and Computer Engineering, University of British Columbia, Vancouver, BC, Canada. He is now with Dyaptive Systems, Vancouver, BC, Canada. L. Lampe is with the Department of Electrical and Computer Engineering, University of British Columbia, Vancouver, BC, Canada. (e-mail: a.kenarsari@gmail.com, Lampe@ece.ubc.ca).

- A closed-form approximation for the PDF of bit-wise reliability metrics when transmitting over nonfading GMN channels and using Euclidean-distance based decoding is derived. The resulting PDF expression is valid for arbitrary signal constellations and labeling rules.
- Based on this new expression, we derive the Laplace transform of the PDF of reliability metrics for general fading GMN channels. Using this result together with the saddlepoint approximation [12], the pairwise error probability (PEP) between codewords can be obtained. For the general GMN case, the saddlepoint needs to be found numerically, which however can be done very efficiently due to the convexity of the Laplace transform [11]. The BER for BICM with linear codes is then readily approximated in terms of these PEP expressions.
- For the special case of fading AWGN channels, for which the Euclidean-distance based metric is maximum likelihood, the PEP is given in closed form. This is a valuable result in its own right, as previous studies have been limited to Nakagami- $m$  fading channels [6], [8], [9].
- We simplify the saddlepoint-based approximation for the high signal-to-noise ratio (SNR) regime, which results in closed-form expressions for asymptotically high SNR. It is shown that the diversity order of the system is the product of the fading diversity order and the minimum Hamming distance of the BICM code. The asymptotic coding gain consists of two terms, one of which is a function of the GMN parameters and the other is a generalization of the harmonic distance obtained in [2], [8].
- In the case of nonfading GMN, where the noise component with the largest power dominates the asymptotic BER, the convergence of the asymptotic BER approximation occurs only at very low BERs for typical GMN scenarios. We therefore also derive a novel closed-form expression for the PEP in nonfading GMN, which takes all mixture-noise components into account and is confirmed to be tight in BER ranges typically of interest.

We present a number of selected numerical results for convolutional coded BICM and different constellations, labeling rules, and fading and noise scenarios, which clearly illustrate the usefulness of the proposed approximations and asymptotic results to predict the BER performance.

The remainder of this paper is organized as follows. In Section II, the BICM transmission model is introduced. The new expressions to analyze the BICM error rate are derived in Section III. In Section IV we provide the simplifications applicable in the high SNR regime. Numerical results obtained from the proposed analytical approximations and simulations are compared and discussed in Section V. Section VI concludes this paper.

## II. SYSTEM MODEL

The block diagram of the equivalent baseband discrete-time BICM transmission system is shown in Figure 1. At the transmitter, the output of a binary encoder  $c = [c_1, c_2, \dots, c_B]$  is first interleaved into  $c^\pi = [c_1^\pi, c_2^\pi, \dots, c_B^\pi]$  and then input to

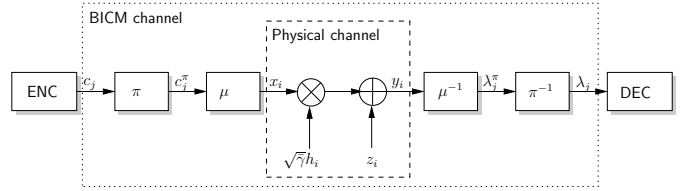


Fig. 1. Block diagram of BICM transmission over a fading channel impaired by Gaussian mixture noise. Also indicated is the binary-input continuous-output equivalent BICM channel.  $\pi$  and  $\pi^{-1}$  denote interleaving and deinterleaving, respectively.  $\mu$  and  $\mu^{-1}$  denote bit-to-symbol mapping and demapping (i.e., bit-metric computation), respectively.

a mapper  $\mu : \{0, 1\}^r \rightarrow \mathcal{X}$  to obtain the transmitted symbol  $x_i = \mu \left[ c_{(i-1)r+1}^\pi, c_{(i-1)r+2}^\pi, \dots, c_{ir}^\pi \right]$  at symbol time  $i$ . The transmitted symbols  $x_i$  are taken from a general complex-valued constellation  $\mathcal{X}$  of size  $2^r$ .

The channel considered in this work is flat fading with additive non-Gaussian noise. Assuming coherent reception, the equivalent discrete-time transmission model can be written as

$$y_i = \sqrt{\gamma} h_i x_i + z_i, \quad (1)$$

where  $y_i \in \mathbb{C}$ ,  $h_i \in \mathbb{R}^+$ , and  $z_i \in \mathbb{C}$  are the  $i$ th received sample, channel gain, and noise sample, respectively. Taking into account the effect of interleaving, the fading gains  $h_i$  are modeled as independent and identically distributed (i.i.d.) random variables with unit power  $\mathbb{E}\{h_i^2\} = 1$ . Similarly, the noise samples are also i.i.d. and distributed according to the zero-mean Gaussian mixture distribution

$$f_Z(z) = \sum_{n=1}^N \frac{\epsilon_n}{2\pi\sigma_n^2} \exp\left(-\frac{\|z\|^2}{2\sigma_n^2}\right), \quad (2)$$

where

$$\sum_{n=1}^N \epsilon_n = 1, \quad (3)$$

$$\sum_{n=1}^N \epsilon_n \sigma_n^2 = \frac{1}{2}, \quad (4)$$

and thus  $\mathbb{E}\{\|z_i\|^2\} = 1$ . Also, without loss of generality, we assume that

$$\sigma_i < \sigma_j, \quad \forall (i, j) \ i > j. \quad (5)$$

The finite-order GMN PDF (2) can well approximate many continuous PDFs and is often used to represent the combined effect of Gaussian background noise and man-made or impulsive noise [15], [16], [17], [18], [19], [20], [21], [14]. We will repeatedly consider the special case of AWGN, for which  $N = 1$  in (2).

Considering the fading and noise power normalizations,  $\bar{\gamma}$  in (1) represents the average SNR at the receiver. We define the instantaneous SNR as

$$\gamma_i \triangleq \bar{\gamma} h_i^2. \quad (6)$$

At the receiver, the demapper outputs  $r$  bitwise reliability

metrics per symbol according to

$$\lambda_{(i-1)r+j}^\pi = - \min_{a \in \mathcal{X}_{j,1}} \left( \|y_i - \sqrt{\gamma} h_i a\|^2 \right) + \min_{a \in \mathcal{X}_{j,0}} \left( \|y_i - \sqrt{\gamma} h_i a\|^2 \right), \quad (7)$$

where  $\mathcal{X}_{j,b}$  is the set of symbols in the constellation with the  $j$ th bit in the binary label fixed to  $b$ . Even though (7) is not the true LLR in the presence of GMN, optimum maximum-likelihood decoding would require the knowledge of noise PDF or the active mixture component (i.e., the noise state  $n$ ) and its variance. Since this knowledge is usually not available at the receiver, the use of the conventional Euclidean distance metric (7) is often considered, e.g. [14]. The ‘‘max-log’’ approximation applied in (7) is appealing from an implementation point of view and has been shown to be effective in Gaussian noise environments [2], [24]. The metrics  $\lambda_j^\pi$  are deinterleaved into  $\lambda_j$ , which are then input to the decoder for the binary code in order to retrieve the binary transmitted data.

We make the common approximation of perfect (i.e., infinite-depth) interleaving, so that the transmission channel between encoder output  $c_j$  and decoder input  $\lambda_j$  can be modeled as an equivalent binary-input output-symmetric (BIOS) channel, which is known as equivalent BICM channel [4] (refer to Figure 1).<sup>1</sup> Since BIOS channel input and output variables are i.i.d., we drop the time index in the following.

### III. ERROR RATE ANALYSIS

In this section, we derive expressions to approximate the BICM BER for fading GMN channels. To this end, we first briefly review the saddlepoint approximation for the PEP [12] (Section III-A) and the approximation of the PDF of reliability metrics developed in [9] (Section III-B). The latter is then extended to the case of GMN (Section III-C), and its Laplace transform for fading GMN channels, which is required for the PEP saddlepoint approximation, is derived (Section III-D).

#### A. BER Estimation

We consider the popular union bound BER estimation [25], which relies on the code’s distance spectrum and expressions for the PEP between two codewords. Assuming a linear code and the BIOS channel with perfect interleaving, the PEP only depends on the Hamming weight  $d_H$  of the corresponding error event and can be expressed as the tail probability of the random variable

$$\Delta_{d_H} \triangleq \sum_{j=1}^{d_H} \Lambda_j, \quad (8)$$

generated by adding  $d_H$  i.i.d. random variables  $\Lambda_j$  which have the same distribution as the reliability metrics (7) when transmitting  $c = 1$ .<sup>2</sup> That is,

$$\text{PEP}(d_H) = \Pr(\Delta_{d_H} < 0). \quad (9)$$

<sup>1</sup>Already for moderate interleaver depths the effect of finite-depth interleaving is only observable at very low SNR [8].

<sup>2</sup>The choice of  $c = 1$  is without loss of generality.

For a closed-form estimation of (9), the saddlepoint approximation

$$\Pr(\Delta_{d_H} < 0) \approx \frac{\exp(d_H \kappa_{\Lambda|f_\gamma}(\hat{s}))}{\hat{s} \sqrt{2\pi d_H \kappa''_{\Lambda|f_\gamma}(\hat{s})}}, \quad (10)$$

has become very popular, e.g. [12], [4], [6]. In (10), we have used the cumulant transform  $\kappa_{\Lambda|f_\gamma}(s)$  of  $-\Lambda_j$  given a fading channel with PDF  $f_\gamma(\gamma)$  for the instantaneous SNR  $\gamma$  defined in (6), and  $\kappa''_{\Lambda|f_\gamma}(s)$  is the second derivative of  $\kappa_{\Lambda|f_\gamma}(s)$ . We have that  $\kappa_{\Lambda|f_\gamma}(s) = \log(\Phi_{\Lambda|f_\gamma}(s))$ , where  $\Phi_{\Lambda|f_\gamma}(s)$  denotes the Laplace transform of the PDF of  $\Lambda_j$ .  $\hat{s} \in (0, s_{\max})$  is known as the saddlepoint, where  $s_{\max} \in \mathbb{R}^+$  denotes the leftmost pole of  $\Phi_{\Lambda|f_\gamma}(s)$ . It is defined through

$$\kappa'_{\Lambda|f_\gamma}(\hat{s}) = \Phi'_{\Lambda|f_\gamma}(\hat{s}) = 0. \quad (11)$$

For BIOS channels with maximum likelihood demapping it is known that  $\hat{s} = 1/2$ , which is also a close approximation for the max-log metric (7) in the case of AWGN [6]. However, for general GMN the saddlepoint deviates significantly from  $1/2$ . In this case, since  $\Phi_{\Lambda|f_\gamma}(s)$  is a convex function [11],  $\hat{s}$  can be determined by fast search methods [26, Ch. 9, 10].

#### B. Previous Result

The following derivations build on the observation from [9] that the PDF of reliability metrics for transmission of  $c = 1$  over the nonfading AWGN channel are well approximated by<sup>3</sup>

$$f_{\Lambda|\gamma}^{\text{QAM}}(\lambda) = \frac{1}{r 2^{r-1}} \sum_{k=1}^5 \sum_{l=1}^{2^{r-1}-1} n_{k,l} f_{\Lambda,k|\gamma,d_l}(\lambda), \quad (12)$$

$$d_l = l d_{\min},$$

for regular QAM constellations and

$$f_{\Lambda|\gamma}^{\text{PSK}}(\lambda) = \frac{1}{r 2^{r-1}} \sum_{l=1}^{2^{r-1}} [n_{1,l} f_{\Lambda,1|\gamma,d_l}(\lambda) + n_{6,l} f_{\Lambda,6|\gamma,d_l,\theta_l}(\lambda)], \quad (13)$$

$$\begin{cases} d_l = [\sin(\frac{\pi l}{2^r}) / \sin(\frac{\pi}{2^r})] d_{\min}, \\ \theta_l = \pi - \frac{2\pi l}{2^r}. \end{cases}$$

for phase-shift keying (PSK) constellations with minimum Euclidean distance  $d_{\min}$ . In (12) and (13),  $f_{\Lambda,k|\gamma,d_l}(\lambda)$  is the PDF of the reliability metric given  $c = 1$  was transmitted considering a subset of ‘‘competitive’’ signal points representing  $c = 0$  at distance  $d_l$ . There are six non-equivalent types of subsets for QAM and PSK constellations and, for convenience, the closed-form expressions for  $f_{\Lambda,k|\gamma,d_l}(\lambda)$  are given in Table I, where  $\mathcal{N}_{\mu,\sigma^2}(x)$  denotes the real-valued Gaussian PDF with mean  $\mu$  and variance  $\sigma^2$ ,  $\text{erf}(x)$  is the Gauss error function, and  $u(x)$  is the unit step function. The coefficient  $n_{k,l}$  denotes the number of subsets of type  $k$  at Euclidean distance  $d_l$ . Table II provides numerical values for  $n_{k,l}$  for a number of popular constellations and labeling rules.

<sup>3</sup>The notation ‘‘ $|\gamma$ ’’ means that the expression is conditioned on the instantaneous SNR  $\gamma$ , while ‘‘ $\cdot|f_\gamma$ ’’ denotes an expression for given SNR distribution  $f_\gamma$ . In the nonfading case, we have  $\gamma = \bar{\gamma}$  and thus the expression conditioned on  $\gamma$  is the final result.

TABLE I  
PROBABILITY DENSITY FUNCTION OF RELIABILITY METRICS,  $f_{\Lambda,k|\gamma,d}(\lambda)$   
AND  $f_{\Lambda,k|\gamma,d,\theta}(\lambda)$ , FOR TRANSMISSION OVER NONFADING AWGN  
CHANNEL, USED IN (12) AND (13).

$k = 1$	$\mathcal{N}_{d^2\gamma,2d^2\gamma}(\lambda)$	
$k = 2$	$\mathcal{N}_{d^2\gamma,2d^2\gamma}(\lambda)$	$1 - \operatorname{erf}\left(\frac{\lambda - d^2\gamma}{2d\sqrt{\gamma}}\right)$
$k = 3$	$2\mathcal{N}_{d^2\gamma,2d^2\gamma}(\lambda)u(d^2\gamma - \lambda)$	
$k = 4$	$\mathcal{N}_{d^2\gamma,2d^2\gamma}(\lambda)$	$1 - 2\operatorname{erf}\left(\frac{\lambda - d^2\gamma}{2d\sqrt{\gamma}}\right)u(d^2\gamma - \lambda)$
$k = 5$	$-4\mathcal{N}_{d^2\gamma,2d^2\gamma}(\lambda)\operatorname{erf}\left(\frac{\lambda - d^2\gamma}{2d\sqrt{\gamma}}\right)u(d^2\gamma - \lambda)$	
$k = 6$	$\mathcal{N}_{d^2\gamma,2d^2\gamma}(\lambda)$	$1 - \operatorname{erf}\left(\tan\left(\frac{\theta}{2}\right)\frac{\lambda - d^2\gamma}{2d\sqrt{\gamma}}\right)$

TABLE II  
VALUES OF THE COEFFICIENTS  $n_{k,l}$  USED IN (12), (13), (17), AND (22)  
FOR A NUMBER OF POPULAR CONSTELLATIONS. Only non-zero coefficients  
are shown. GRAY LABELING (GL), SET PARTITIONING LABELING (SPL),  
MODIFIED SET PARTITIONING LABELING (MSPL), MIXED LABELING  
(ML), AND SEMI SET PARTITIONING LABELING (SSPL), CF. [31] [32].

4QAM	GL	$n_{1,1} = 4$
	SPL	$n_{1,1} = 2, n_{2,1} = 2$
16QAM	GL	$n_{1,1} = 24, n_{1,2} = 8$
	SPL	$n_{1,1} = 8, n_{1,2} = 4, n_{2,1} = 10,$ $n_{3,1} = 4, n_{4,1} = 4, n_{5,1} = 2$
	MSPL	$n_{1,1} = 16, n_{2,1} = 4, n_{2,2} = 2,$ $n_{3,1} = 4, n_{4,1} = 4, n_{5,1} = 2$
	ML	$n_{1,1} = 24, n_{3,1} = 8$
64QAM	GL	$n_{1,1} = 112, n_{1,2} = 48,$ $n_{1,3} = 16, n_{1,4} = 16$
	GL	$n_{1,1} = 8, n_{1,2} = 4$
8PSK	GL	$n_{1,1} = 8, n_{1,2} = 4$
	SPL	$n_{1,1} = 6, n_{1,2} = 2, n_{2,1} = 4$
	SSPL	$n_{1,1} = 6, n_{2,1} = 6$

### C. Extension of PDF Result to Nonfading GMN

We note that the PDF approximation developed in [9] is applicable to arbitrary signal constellations, including, for example, PSK with non-uniformly spaced signal points and amplitude phase-shift keying (APSK) [27] constellations. The resulting PDF expressions have the same form as those in (12) and (13), with appropriately modified numerical values for  $n_{k,l}$ ,  $d_l$ , and  $\theta_l$ . In the following, we therefore use the general expression

$$f_{\Lambda|\gamma}(\lambda) = \frac{1}{r^{2r-1}} \sum_{k \in \mathcal{K}} \sum_{l=1}^M n_{k,l} f_{\Lambda,k|\gamma,\eta_l}(\lambda), \quad (14)$$

where  $\mathcal{K}$  is the set of non-equivalent types,  $M$  is the maximal number of non-zero coefficients  $n_{k,l}$ , and  $\eta_l$  denotes the constellation parameters. For example,  $\mathcal{K} = \{1, \dots, 5\}$ ,  $M = 2^{r-1} - 1$ , and  $\eta_l = d_l$  for QAM, and  $\mathcal{K} = \{1, 6\}$ ,  $M = 2^{r-1}$ , and  $\eta_l = [d_l, \theta_l]$  for PSK.

In order to extend (14) to the case of GMN, we introduce the auxiliary random variable  $\xi_i$  which identifies to which component  $n$  of the PDF (2)  $z_i$  belongs. The ‘‘noise-state’’ variable  $\xi_i$  is i.i.d. with distribution  $\Pr\{\xi_i = n\} = \epsilon_n$ .

Instead of directly using the PDF of GMN for performance analysis, we use  $\xi_i$  to define the component-noise random variable  $Z^{\xi_i}$  with

$$p_{Z^n}(z) = \frac{1}{2\pi\sigma_n^2} \exp\left(-\frac{\|z\|^2}{2\sigma_n^2}\right). \quad (15)$$

Then, the PDF of reliability metrics can be considered as a weighted sum of PDFs  $f_{\Lambda|\gamma,n}(\lambda)$  conditioned on the state of GMN  $\xi_i = n$ ,

$$f_{\Lambda|\gamma}(\lambda) = \sum_{n=1}^N \epsilon_n f_{\Lambda|\gamma,n}(\lambda), \quad (16)$$

where  $f_{\Lambda|\gamma,n}(\lambda)$  is expressed analogous to (14) as

$$f_{\Lambda|\gamma,n}(\lambda) = \frac{1}{r^{2r-1}} \sum_{k \in \mathcal{K}} \sum_{l=1}^M n_{k,l} f_{\Lambda,k|\gamma,n,\eta_l}(\lambda). \quad (17)$$

Since  $f_{\Lambda,k|\gamma,n,\eta_l}(\lambda)$  is conditioned on  $\xi_i = n$ , one may be inclined to obtain its PDF by replacing the instantaneous SNR  $\gamma$  with  $\gamma/(2\sigma_n^2)$  in the expressions for  $f_{\Lambda,k|\gamma,\eta_l}(\lambda)$  in Table I (recall the normalization  $\sum_{n=1}^N \epsilon_n \sigma_n^2 = 1/2$ ). This would indeed be correct, if the receiver had knowledge about the instantaneous noise state  $\xi_i$ , which however is not the case for the conventional demapper (7) considered here. A proper derivation of  $f_{\Lambda,k|\gamma,n,\eta_l}(\lambda)$  following the steps in [9] leads to the closed-form expressions presented in Table III (top part).

We observe that the resulting PDF expression (16) using (17) and the results in Table III is very easy to evaluate, and its computation does not require any numerical integration.

### D. Laplace Transform of the PDF of Reliability Metrics for Fading GMN

Using the PDF expression (16), we now proceed to derive expressions for the Laplace transform  $\Phi_{\Lambda|f_\gamma}(s)$ , which is required for the PEP saddlepoint approximation (10). We will assume  $s \in \mathbb{R}^+$ , which is sufficient for evaluation of (10).

Using the fact that PDF of reliability metrics for fading channels can be expressed as

$$f_{\Lambda|f_\gamma}(\lambda) = \int_0^\infty f_\gamma(\gamma) f_{\Lambda|\gamma}(\lambda) d\gamma, \quad (18)$$

we write the Laplace transform

$$\begin{aligned} \Phi_{\Lambda|f_\gamma}(s) &= \int_{-\infty}^\infty f_{\Lambda|f_\gamma}(\lambda) \exp(-s\lambda) d\lambda \\ &= \int_0^\infty f_\gamma(\gamma) \left[ \int_{-\infty}^\infty f_{\Lambda|\gamma}(\lambda) \exp(-s\lambda) d\lambda \right] d\gamma \\ &\triangleq \int_0^\infty f_\gamma(\gamma) \Phi_{\Lambda|\gamma}(s) d\gamma, \end{aligned} \quad (19)$$

where we changed the order of integration (assuming  $s$  is such that  $\Phi_{\Lambda|f_\gamma}(s)$  exists) and defined  $\Phi_{\Lambda|\gamma}(s)$  as the Laplace

TABLE III

EXPRESSIONS FOR (I) PDF OF RELIABILITY METRICS,  $f_{\Lambda,k|\gamma,n,\eta}(\lambda)$ , FOR TRANSMISSION OVER NONFADING GMN CHANNEL, USED IN (17), (II) ITS LAPLACE TRANSFORM  $\Phi_{\Lambda,k|\gamma,n,\eta}(s)$  USED IN (22), AND (III) THE LAPLACE TRANSFORM  $\Phi_{\Lambda,k|f_\gamma,n,\eta}(s)$  FOR FADING GMN CHANNELS AS FUNCTION OF MGF  $M_{f_\gamma}(s)$  (27) AND THE FINITE-SERIES EXPRESSIONS  $S_1(s; \omega, \nu, \rho)$  (28) AND  $S_2(s; \omega, \nu, \rho)$  (29).  $s \in \mathbb{R}^+$ ,  $\eta = d$  FOR  $k = 1, \dots, 5$ , AND  $\eta = [d, \theta]$  FOR  $k = 6$ .

PDF $f_{\Lambda,k \gamma,n,\eta}(\lambda)$	
$k = 1$	$\mathcal{N}_{d^2\gamma, 4\sigma_n^2 d^2\gamma}(\lambda)$
$k = 2$	$\mathcal{N}_{d^2\gamma, 4\sigma_n^2 d^2\gamma}(\lambda) \left  1 - \operatorname{erf} \left( \frac{\lambda - d^2\gamma}{2\sqrt{2}\sigma_n d\sqrt{\gamma}} \right) \right $
$k = 3$	$2\mathcal{N}_{d^2\gamma, 4\sigma_n^2 d^2\gamma}(\lambda) u(d^2\gamma - \lambda)$
$k = 4$	$\mathcal{N}_{d^2\gamma, 4\sigma_n^2 d^2\gamma}(\lambda) \left  1 - 2\operatorname{erf} \left( \frac{\lambda - d^2\gamma}{2\sqrt{2}\sigma_n d\sqrt{\gamma}} \right) \right  u(d^2\gamma - \lambda)$
$k = 5$	$-4\mathcal{N}_{d^2\gamma, 4\sigma_n^2 d^2\gamma}(\lambda) \operatorname{erf} \left( \frac{\lambda - d^2\gamma}{2\sqrt{2}\sigma_n d\sqrt{\gamma}} \right) u(d^2\gamma - \lambda)$
$k = 6$	$\mathcal{N}_{d^2\gamma, 4\sigma_n^2 d^2\gamma}(\lambda) \left  1 - \operatorname{erf} \left( \tan \left( \frac{\theta}{2} \right) \frac{\lambda - d^2\gamma}{2\sqrt{2}\sigma_n d\sqrt{\gamma}} \right) \right $
Laplace transform $\Phi_{\Lambda,k \gamma,n,\eta}(s)$	
$k = 1$	$\exp(d^2\gamma(2\sigma_n^2 s^2 - s))$
$k = 2$	$\exp(d^2\gamma(2\sigma_n^2 s^2 - s)) (1 + \operatorname{erf}(\sigma_n d\sqrt{\gamma}s))$
$k = 3$	$\exp(d^2\gamma(2\sigma_n^2 s^2 - s)) (1 + \operatorname{erf}(\sqrt{2}\sigma_n d\sqrt{\gamma}s))$
$k = 4$	$\frac{1}{2} \exp(d^2\gamma(2\sigma_n^2 s^2 - s)) (1 + \operatorname{erf}(\sqrt{2}\sigma_n d\sqrt{\gamma}s) + (1 + \operatorname{erf}(\sigma_n d\sqrt{\gamma}s))^2)$
$k = 5$	$\exp(d^2\gamma(2\sigma_n^2 s^2 - s)) (1 + \operatorname{erf}(\sigma_n d\sqrt{\gamma}s))^2$
$k = 6$	$\exp(d^2\gamma(2\sigma_n^2 s^2 - s)) (1 + \operatorname{erf}(\sin(\frac{\theta}{2})\sqrt{2}\sigma_n d\sqrt{\gamma}s))$
Laplace transform $\Phi_{\Lambda,k f_\gamma,n,\eta}(s)$	
$k = 1$	$M_{f_\gamma}(d^2(2\sigma_n^2 s^2 - s))$
$k = 2$	$M_{f_\gamma}(d^2(2\sigma_n^2 s^2 - s)) + S_1(s; 2\sigma_n^2 d^2, d^2, \sigma_n d)$
$k = 3$	$M_{f_\gamma}(d^2(2\sigma_n^2 s^2 - s)) + S_1(s; 2\sigma_n^2 d^2, d^2, \sqrt{2}\sigma_n d)$
$k = 4$	$M_{f_\gamma}(d^2(2\sigma_n^2 s^2 - s)) + \frac{1}{2}S_1(s; 2\sigma_n^2 d^2, d^2, \sqrt{2}\sigma_n d) + S_1(s; 2\sigma_n^2 d^2, d^2, \sigma_n d) + \frac{1}{2}S_2(s; 2\sigma_n^2 d^2, d^2, \sigma_n d)$
$k = 5$	$M_{f_\gamma}(d^2(2\sigma_n^2 s^2 - s)) + 2S_1(s; 2\sigma_n^2 d^2, d^2, \sigma_n d) + S_2(s; 2\sigma_n^2 d^2, d^2, \sigma_n d)$
$k = 6$	$M_{f_\gamma}(d^2(2\sigma_n^2 s^2 - s)) + S_1(s; 2\sigma_n^2 d^2, d^2, \sqrt{2}\sin(\frac{\theta}{2})\sigma_n d)$

transform of  $f_{\Lambda|\gamma}(\lambda)$ . From (16), (17), and the linearity property of the Laplace transform we have

$$\Phi_{\Lambda|\gamma}(s) = \sum_{n=1}^N \epsilon_n \Phi_{\Lambda|\gamma,n}(s), \quad (21)$$

where

$$\Phi_{\Lambda|\gamma,n}(s) = \frac{1}{r2^{r-1}} \sum_{k \in \mathcal{K}} \sum_{l=1}^M n_{k,l} \Phi_{\Lambda,k|\gamma,n,\eta_l}(s) \quad (22)$$

and  $\Phi_{\Lambda,k|\gamma,n,\eta_l}(s)$  is the Laplace transform of  $f_{\Lambda,k|\gamma,n,\eta_l}(\lambda)$ . Considering the expressions for  $f_{\Lambda,k|\gamma,n,\eta_l}(\lambda)$  in Table III and using the integration technique presented in [9, Appendices 1 and 2], closed-form expressions for  $\Phi_{\Lambda,k|\gamma,n,\eta_l}(s)$  are obtained, which are summarized in Table III (middle part). These results together with (22) and (21) give us closed-form expressions for  $\Phi_{\Lambda|\gamma}(s)$ , which allows us to evaluate the saddlepoint approximation (10) for nonfading GMN channels. For fading GMN channels we define

$$\Phi_{\Lambda,k|f_\gamma,n,\eta_l}(s) \triangleq \int_0^\infty f_\gamma(\gamma) \Phi_{\Lambda,k|\gamma,n,\eta_l}(s) d\gamma, \quad (23)$$

and it follows from (20), (21), and (22) that

$$\Phi_{\Lambda|f_\gamma}(s) = \frac{1}{r2^{r-1}} \sum_{n=1}^N \epsilon_n \sum_{k \in \mathcal{K}} \sum_{l=1}^M n_{k,l} \Phi_{\Lambda,k|f_\gamma,n,\eta_l}(s). \quad (24)$$

Applying the methods from [9, Appendices 3 and 4], the integral in (23) can be solved in closed form with elementary function for Nakagami- $m$  fading channels with integer parameter  $m$ , and in terms of hypergeometric functions for non-integer  $m$ . However, no closed-form solution exists for other popular fading distributions like Nakagami- $n$  or Nakagami- $q$ . Therefore, we propose the use of the approximations

$$\operatorname{erf}(x) \approx P(x) \triangleq \sum_{i=1}^K a_i \exp(b_i x^2), \quad (25)$$

$$(\operatorname{erf}(x))^2 \approx \bar{P}(x) \triangleq \sum_{i=1}^{\bar{K}} \bar{a}_i \exp(\bar{b}_i x^2), \quad (26)$$

with coefficients  $a_i$ ,  $b_i$ ,  $\bar{a}_i$ ,  $\bar{b}_i$  and number of terms  $K$ ,  $\bar{K}$  chosen according to the particular approximation method and required accuracy. Such approximations for the error function can be obtained using the alternative representation of the Gaussian  $Q$ -function and approximation of the integral using a

TABLE IV  
THE MGF OF SNR  $M_{f_\gamma}(s)$  AND ITS ASYMPTOTIC FORM  $M_{f_\gamma}^a(s)$  FOR A  
NUMBER OF POPULAR FADING DISTRIBUTIONS, CF. [29].

Fading model	$M_{f_\gamma}(s)$	$M_{f_\gamma}^a(s)$
Rayleigh	$(1 - s\bar{\gamma})^{-1}$	$-\frac{1/s}{\bar{\gamma}}$
Nakagami- $m$	$\left(1 - \frac{s\bar{\gamma}}{m}\right)^{-m}$	$\frac{m^m/(-s)^m}{\bar{\gamma}^m}$
Nakagami- $n$	$\frac{(1+n^2)}{(1+n^2) - s\bar{\gamma}} \times \exp\left(\frac{n^2 s \bar{\gamma}}{(1+n^2) - s\bar{\gamma}}\right)$	$-\frac{(1+n^2)}{\bar{\gamma}} \times \exp(-n^2)/s$
Nakagami- $q$	$\left(1 - 2s\bar{\gamma} + \frac{(2s\bar{\gamma})^2 q^2}{(1+q^2)^2}\right)^{-0.5}$	$-\frac{1+q^2/s}{\bar{\gamma}}$

Riemann sum, cf. [28]. Equipped with (25), (26), and defining the moment generating function (MGF) of the instantaneous SNR  $\gamma$

$$M_{f_\gamma}(s) \triangleq \int_0^\infty f_\gamma(t) \exp(st) dt, \quad (27)$$

as well as the finite series

$$S_1(s; \omega, \nu, \rho) \triangleq \sum_{i=1}^K a_i M_{f_\gamma}(-\nu s + (\omega + b_i \rho^2) s^2), \quad (28)$$

$$S_2(s; \omega, \nu, \rho) \triangleq \sum_{i=1}^{\bar{K}} \bar{a}_i M_{f_\gamma}(-\nu s + (\omega + \bar{b}_i \rho^2) s^2), \quad (29)$$

the resulting expressions for  $\Phi_{\Lambda, k|f_\gamma, n, \eta_l}(s)$  are presented in Table III (bottom part).

Hence a simple closed-form approximation of  $\Phi_{\Lambda|f_\gamma}(s)$  for fading GMN channels is obtained as long as the MGF of the SNR is available in closed form, which is the case for almost all the practical fading distributions [29]. Table IV (second column) summarizes the formulas for  $M_{f_\gamma}(s)$  for the most popular fading models.

#### IV. ANALYSIS IN THE HIGH-SNR REGIME

In this section, we consider the high-SNR regime to obtain further simplified expressions for the PEP. We first consider the nonfading GMN channel (where  $\bar{\gamma} = \gamma$ ) and derive the PEP saddlepoint approximation for high SNR. Since the saddlepoint analysis does not result in a fully analytical solution (the numerical search for the saddlepoint remains), we also derive an alternative BER expression, which does not rely on the saddlepoint approximation. For general fading channels, we consider the PEP saddlepoint approximation for the case of asymptotically high SNR, which leads us to expressions for the coding and diversity gain for BICM transmission. To make explicit that the analysis in this chapter uses high-SNR approximations which become accurate for asymptotically high SNR, we apply the superscript ‘‘a’’ to the respective variables.

#### A. Simplified Expression for PDF of Reliability Metric and Its Laplace Transform

In the case of high SNR, the PDF expressions in Table III can be well approximated by

$$f_{\Lambda, k|\gamma, n, d_l}^a(\lambda) = c_k \mathcal{N}_{d_l^2 \gamma, 4\sigma_n^2 d_l^2 \gamma}(\lambda), \quad (30)$$

where  $[c_1, c_2, c_3, c_4, c_5, c_6] = [1, 2, 2, 3, 4, 2]$ , and thus the PDF expression given in (16) simplifies to

$$f_{\Lambda|\gamma}^a(\lambda) = \sum_{n=1}^N \epsilon_n \left[ \sum_{l=1}^M N_l \mathcal{N}_{d_l^2 \gamma, 4\sigma_n^2 d_l^2 \gamma}(\lambda) \right], \quad (31)$$

where  $N_l = \frac{1}{r^{2r-1}} \sum_{k \in \mathcal{K}} c_k n_{k,l}$  can be interpreted as the average number of competitive signal points at distance  $d_l$ . The Laplace transform of  $f_{\Lambda|\gamma}^a(\lambda)$  is given by

$$\Phi_{\Lambda|\gamma}^a(s) = \sum_{n=1}^N \epsilon_n \left[ \sum_{l=1}^M N_l \exp(d_l^2 \gamma (2\sigma_n^2 s^2 - s)) \right], \quad (32)$$

and its average with respect to the instantaneous SNR for fading channels is obtained as

$$\Phi_{\Lambda|f_\gamma}^a(s) = \sum_{n=1}^N \epsilon_n \left[ \sum_{l=1}^M N_l M_{f_\gamma}(d_l^2 (2\sigma_n^2 s^2 - s)) \right]. \quad (33)$$

#### B. Nonfading GMN Channel

1) *Saddlepoint Analysis*: From the Laplace transform expression in (32) we find the saddlepoint  $\hat{s}$  as the (unique) solution of (see (11))

$$\begin{aligned} & \frac{d}{ds} \Phi_{\Lambda|\gamma}^a(s) \\ &= \sum_{n=1}^N \epsilon_n \left[ \sum_{l=1}^M N_l d_l^2 \gamma (4\sigma_n^2 s - 1) \exp(d_l^2 \gamma (2\sigma_n^2 s^2 - s)) \right] \\ &= 0, \end{aligned} \quad (34)$$

from which we infer that  $1/\sigma_1^2 < 4\hat{s} < 1/\sigma_N^2$ . Hence, a numerical search for  $\hat{s}$  in  $(1/(4\sigma_1^2), 1/(4\sigma_N^2))$  is required.

In asymptotically high SNR  $\gamma \rightarrow \infty$ , all terms  $(2\sigma_n^2 s^2 - s)$  need to be negative and thus the term for  $n = 1$  and  $l = 1$  dominates the sum in (34), since  $d_1^2 (2\sigma_1^2 s^2 - s) = \max_{l,n} \{d_l^2 (2\sigma_n^2 s^2 - s)\}$ . Hence, the saddlepoint approaches the solution

$$\lim_{\gamma \rightarrow \infty} \hat{s} = \frac{1}{4\sigma_1^2} \quad (35)$$

and the PEP asymptotic approximation

$$\text{PEP}^a(d_H) = \frac{(\epsilon_1 N_1)^{d_H}}{d_1 \sigma_1 \sqrt{2\pi d_H \gamma}} \exp\left(-\frac{d_H d_1^2}{8\sigma_1^2} \gamma\right) \quad (36)$$

is obtained from (10). We observe that the asymptotic PEP is the same as the PEP for binary transmission with an equivalent SNR of  $(d_H d_1^2 \gamma)/(2\sigma_1^2)$ , scaled by a constant which is a function of the Hamming distance, mapping rule, and GMN parameter  $\epsilon_1$  associated with the component with the largest variance. Due to the multiplicative term  $\epsilon_1^{d_H}$ , we expect (36) to be relevant only for very low BERs in most practical

cases, since the probability of the impulsive components is typically relatively low, cf. e.g. [15], [16], [17], [18], [19], [20], [21], [14]. Therefore, next we present a different expression for the PEP in high SNRs which includes all mixture noise components.

2) *Direct Analysis*: We again start from the expression for Laplace transform of reliability metrics given in (31), and compute the Laplace transform of the PDF of  $\Delta_{d_H}$  defined in (8). Due to the perfect interleaving assumption we obtain

$$\begin{aligned}
\Phi_{\Delta_{d_H}|\gamma}^a(s) &= \left[ \Phi_{\Lambda|\gamma}^a(s) \right]^{d_H} \quad (37) \\
&\stackrel{(a)}{=} \sum_{\substack{n_1, \dots, n_N \\ n_1 + \dots + n_N = d_H}} \frac{d_H!}{\left[ \prod_{i=1}^N (n_i! / \epsilon_i^{n_i}) \right]} \\
&\quad \times \prod_{i=1}^N \left[ \sum_{l=1}^M N_l \exp(d_l^2 \gamma (2\sigma_i^2 s^2 - s)) \right]^{n_i} \\
&\stackrel{(b)}{=} \sum_{\substack{n_1, \dots, n_N \\ n_1 + \dots + n_N = d_H}} \frac{d_H!}{\left[ \prod_{i=1}^N (n_i! / \epsilon_i^{n_i}) \right]} \\
&\quad \times \prod_{i=1}^N \sum_{\substack{l_1, \dots, l_M \\ l_1 + \dots + l_M = n_i}} \frac{n_i!}{\left[ \prod_{j=1}^M (l_j! / N_j^{l_j}) \right]} \\
&\quad \times \exp \left( \sum_{j=1}^M l_j d_j^2 \gamma (2\sigma_i^2 s^2 - s) \right) \\
&= \sum_{\substack{n_1, \dots, n_N \\ n_1 + \dots + n_N = d_H}} \frac{d_H!}{\left[ \prod_{i=1}^N (n_i! / \epsilon_i^{n_i}) \right]} \\
&\quad \times \sum_{\substack{l_{1,1}, \dots, l_{1,M} \\ l_{1,1} + \dots + l_{1,M} = n_1}} \dots \sum_{\substack{l_{N,1}, \dots, l_{N,M} \\ l_{N,1} + \dots + l_{N,M} = n_N}} \prod_{i=1}^N \prod_{j=1}^M \frac{n_i! N_j^{l_{i,j}}}{l_{i,j}!} \\
&\quad \times \exp \left( \sum_{i=1}^N \sum_{j=1}^M l_{i,j} d_j^2 \gamma (2\sigma_i^2 s^2 - s) \right), \quad (38)
\end{aligned}$$

where we applied the multinomial series expansion in (a) and (b). From (38) we observe that the PDF of  $\Delta_{d_H}$  is a superposition of Gaussian PDFs and thus we can directly evaluate (9) as

$$\begin{aligned}
\text{PEP}(d_H) &= \sum_{\substack{n_1, \dots, n_N \\ n_1 + \dots + n_N = d_H}} \frac{d_H!}{\left[ \prod_{i=1}^N (n_i! / \epsilon_i^{n_i}) \right]} \\
&\quad \times \sum_{\substack{l_{1,1}, \dots, l_{1,M} \\ l_{1,1} + \dots + l_{1,M} = n_1}} \dots \sum_{\substack{l_{N,1}, \dots, l_{N,M} \\ l_{N,1} + \dots + l_{N,M} = n_N}} \prod_{i=1}^N \prod_{j=1}^M \frac{n_i! N_j^{l_{i,j}}}{l_{i,j}!} \\
&\quad \times Q \left( \frac{\sqrt{\gamma} \sum_{i=1}^N \sum_{j=1}^M l_{i,j} d_j^2}{2 \sqrt{\sum_{i=1}^N \sum_{j=1}^M l_{i,j} d_j^2 \sigma_i^2}} \right). \quad (39)
\end{aligned}$$

This is a closed-form result for the PEP for transmission over nonfading GMN channels with high SNR. We note that for

the asymptotic case  $\gamma \rightarrow \infty$ , where the term with the largest argument of the Q-function dominates the sum, it can be shown that (39) converges to (36). However, as noted above, this asymptotic result is of interest only for very low BERs.

### C. Fading GMN Channels

In the case of fading channels, we consider the case of asymptotically high SNR  $\bar{\gamma}$  and assume that the MGF of the instantaneous SNR  $M_{f_\gamma}(s)$  can be expressed as

$$M_{f_\gamma}^a(s) = \frac{\alpha}{(-s)^g \bar{\gamma}^g}, \quad (40)$$

where  $\alpha > 0$  and the diversity order  $g > 0$  depend on the fading distribution, cf. [30, AS3]. For integer  $g$ , (40) can be considered as the first term of the Maclaurin series expansion of  $M_{f_\gamma}(s)$  in  $1/\bar{\gamma}$ . Table IV (third column) presents the respective expressions for  $M_{f_\gamma}^a(s)$  for a number of popular fading distributions. Substituting (40) into (33) we have

$$\begin{aligned}
\Phi_{\Lambda|f_\gamma}^a(s) &= \sum_{n=1}^N \epsilon_n \left[ \sum_{l=1}^M \frac{N_l \alpha}{(d_l^2 (s - 2\sigma_n^2 s^2))^g \bar{\gamma}^g} \right] \\
&= \left[ \sum_{l=1}^M \frac{\alpha N_l}{d_l^{2g}} \right] \left[ \sum_{n=1}^N \frac{\epsilon_n}{(s - 2\sigma_n^2 s^2)^g} \right] \frac{1}{\bar{\gamma}^g}. \quad (41)
\end{aligned}$$

Therefore, the asymptotic saddlepoint is the (unique) solution of

$$\sum_{n=1}^N \frac{\epsilon_n (4\sigma_n^2 s - 1)}{(1 - 2\sigma_n^2 s)^{g+1}} = 0, \quad (42)$$

which cannot be given in closed form. However, we note that the saddlepoint only depends on the GMN parameters and diversity order  $g$  of the fading process. We can further limit the numerical search interval considering that  $s_{\max} = 1/(2\sigma_1^2)$  is the leftmost pole of the Laplace transform (41) and that (42) is negative for  $s \leq 1/(4\sigma_1^2)$ . Hence, we get the lower and upper limit

$$\frac{1}{4\sigma_1^2} < \hat{s} < \frac{1}{2\sigma_1^2}. \quad (43)$$

In order to arrive at a closed-form approximation, we may consider the midpoint of the above interval,

$$\hat{s}_e = \frac{3}{8\sigma_1^2}, \quad (44)$$

as an estimate for the asymptotic saddlepoint.

Given the saddlepoint  $\hat{s}$ , defining

$$\zeta(s) \triangleq \sum_{n=1}^N \frac{\epsilon_n}{(4[s - 2\sigma_n^2 s^2])^g}, \quad (45)$$

and substituting (41) into (10), we obtain after some simplifications the asymptotic PEP expression

$$\text{PEP}^a(d_H) = \frac{(\zeta(\hat{s}))^{d_H+1/2}}{\hat{s} \sqrt{2\pi d_H \zeta''(\hat{s})}} \left[ \sum_{l=1}^M \frac{\alpha N_l}{\left(\frac{d_l^2}{4}\right)^g} \right]^{d_H} \frac{1}{\bar{\gamma}^{d_H g}}. \quad (46)$$

We observe that the diversity gain for BICM transmission over fading GMN channels is given by the product  $d_H g$ . The coding

gain consists of two terms, where the first one depends on the GMN parameters through  $\zeta(s)$  (45). The second term

$$\left[ \sum_{l=1}^M \frac{\alpha N_l}{\left(\frac{d^2}{4}\right)^g} \right], \quad (47)$$

depends on the signal constellation and labeling, and can be considered as a generalization of the harmonic distance for BICM with Gray labeling obtained in [2] and [8] for Rayleigh and Nakagami- $m$  fading, respectively.

In the special case of fading AWGN channels, for which  $\hat{s} = 1/2$ , (46) simplifies to

$$\text{PEP}^a(d_H) = \frac{1}{2\sqrt{\pi}d_H g} \left[ \sum_{l=1}^M \frac{\alpha N_l}{\left(\frac{d^2}{4}\right)^g} \right]^{d_H} \frac{1}{\bar{\gamma}^{d_H g}}, \quad (48)$$

which is a generalization of the asymptotic result in [9] for Nakagami- $m$  fading channels.

## V. NUMERICAL RESULTS AND DISCUSSION

In this section, we present and discuss a number of exemplary numerical results to illustrate the accuracy of the proposed PDF and PEP approximations (cf. Sections III-C, III-D, and IV). For this purpose, we use the PEP expressions in the BER union bound for a convolutional code of rate  $R_c = k_c/n_c$ , which is given by [25]

$$P_b \leq \frac{1}{k_c} \sum_{d_H=d_{\text{free}}}^{\infty} w_{d_H} \text{PEP}(d_H), \quad (49)$$

where  $d_{\text{free}}$  denotes the free distance of the convolutional code and  $w_{d_H}$  denotes the total input weight of error events at Hamming distance  $d_H$ .

### A. Parameters

For the BER results we assume BICM with the popular 64-state rate-1/2 convolutional code with generator polynomials  $(171, 133)_8$  and  $d_{\text{free}} = 10$ . The union bound (49) is truncated to  $d_H \leq 25$ . To evaluate the series terms  $S_1(s; \cdot)$  (28) and  $S_2(s; \cdot)$  (29) needed in Table III, we use the error-function approximation (cf. (25) and (26)) [28]

$$P(x) = 1 - \frac{1}{6} \exp(-x^2) - \frac{1}{2} \exp\left(-\frac{4x^2}{3}\right), \quad (50)$$

$$\bar{P}(x) = P^2(x).$$

Furthermore, we consider the following labeling rules: Gray labeling (GL), set partitioning labeling (SPL), modified set partitioning labeling (MSPL), semi set partitioning labeling (SSPL), and mixed labeling (ML) [31], [32]. While GL is of importance when used with non-iterative decoders [2], the other labelings are of practical and theoretical importance for the case of, e.g., BICM transmission with iterative decoding [31], [32], for which our analytical results would provide an approximation of BER after the first decoding iteration and facilitate the selection of the labeling rule.

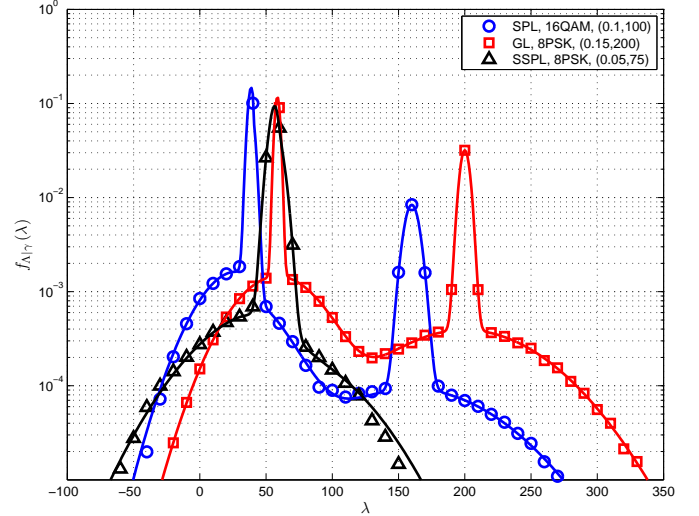


Fig. 2. PDF of reliability metrics for BICM transmission over nonfading channel impaired by  $\epsilon$ -mixture noise with parameters  $(\epsilon, \kappa)$  for different constellations, labeling, and noise parameters. Solid lines represent the PDF approximation given in (16), while markers represent the simulated histograms.

The BER results for different constellations are presented as function of the bit-wise SNR

$$\gamma_b \triangleq \gamma / (R_c r), \quad \bar{\gamma}_b \triangleq \bar{\gamma} / (R_c r). \quad (51)$$

Finally, we consider  $\epsilon$ -mixture noise, which is an important instance of general GMN with two terms, e.g., [17]. The first term represents impulsive noise due to some ambient phenomenon, while the second term accounts for Gaussian background noise. The  $\epsilon$ -mixture noise parameters can be expressed as

$$\begin{aligned} \epsilon_1 &= \epsilon, \quad \epsilon_2 = 1 - \epsilon, \\ \sigma_1 &= \sqrt{\kappa} / \left( \sqrt{2(1 + \kappa\epsilon - \epsilon)} \right), \\ \sigma_2 &= 1 / \left( \sqrt{2(1 + \kappa\epsilon - \epsilon)} \right), \end{aligned} \quad (52)$$

where  $\kappa = \sigma_1^2 / \sigma_2^2$  is a measure for the strength of the impulsive component compared to the thermal noise. In the following, we specify the parameters of  $\epsilon$ -mixture noise by  $(\epsilon, \kappa)$ .

### B. Results

1) *PDF Approximation Results:* Figure 2 shows a comparison of PDF histograms, obtained through Monte Carlo simulation, and the approximation (16) for different constellations, labeling, and noise parameters. The SNR  $\gamma = \bar{\gamma} = 20$  dB is adjusted for these results. We observe that the proposed approximation is very accurate in all cases. In particular, the negative tail of the PDF (i.e.,  $\lambda < 0$ ) is faithfully matched, which is critical for performance evaluation.

2) *BER Results for Nonfading GMN Channels:* Figure 3 shows the analytical (lines) and simulated (markers) BER results for two different constellations and labeling rules assuming transmission over the nonfading channel impaired by  $\epsilon$ -mixture noise. The figure includes (i) the BER union

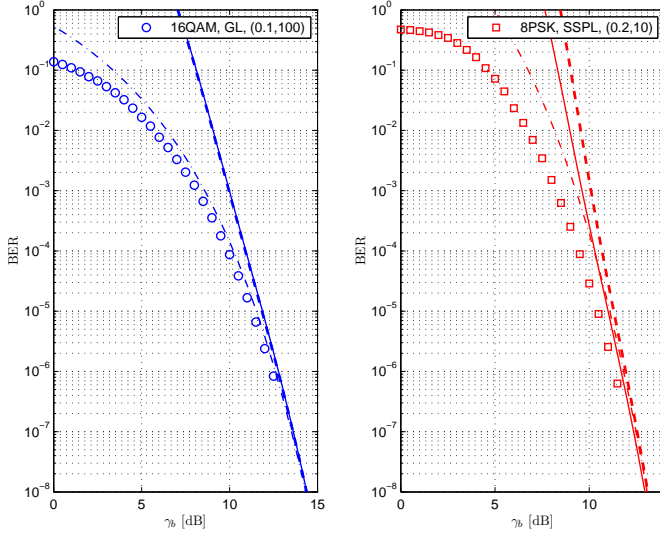


Fig. 3. BER of BICM transmission over a nonfading channel impaired by  $\epsilon$ -mixture noise with parameters  $(\epsilon, \kappa)$  for a 64-state convolutional code of rate 1/2. Solid lines: BER union bound using the saddlepoint approximation (10). The saddlepoint is found numerically for each SNR. Dashed lines: BER union bound using the PEP expression for high SNR in (39). Dash-dotted lines: BER using only the PEP expression in (39) for  $d_H = d_{\text{free}}$ . Markers are simulation results.

bound (49) with the saddlepoint approximation (10) using the saddlepoint found numerically for each SNR (solid lines), (ii) the the BER union bound (49) using the PEP expression for high SNR in (39) (dashed lines), and (iii) the PEP expression in (39) for  $d_H = d_{\text{free}}$  (dash-dotted lines). It can be seen that the BER union bound is fairly tight for both BICM examples. Likewise, the closed-form expression (39) provides very good BER approximations and the curves converge to those from the non-asymptotic saddlepoint analysis. Considering only the PEP from (39) for the minimum Hamming distance term enables a quick and fairly accurate BER estimation. We note that the asymptotic saddlepoint approximation (36) (not shown in this figure) becomes tight only for BERs below  $\epsilon^{d_{\text{free}}}$ , and thus it is more useful for codes with lower  $d_{\text{free}}$  and  $\epsilon$ -mixture noise with high probability of impulses.

3) *BER Results for Fading AWGN Channels:* Next we consider BER results for BICM transmission over fading AWGN channels (i.e.,  $\epsilon = 1$ ) with different constellations and labeling rules. Specifically, Nakagami- $m$  and Nakagami- $n$  fading distributions are applied. Figure 4 shows BER curves obtained from the BER union bound using the saddlepoint approximation (lines) together with simulation results (markers). For the former, both the actual saddlepoint, which has been determined numerically (dashed lines), and the approximation  $\hat{s} = 1/2$  (solid lines) has been used. We observe a very good match between results from analysis and simulations. In particular, since for AWGN the applied decoding metric is almost the maximum-likelihood metric (note that the max-log approximation is used in (7)), the difference between the results using the true saddlepoint  $\hat{s}$  and  $\hat{s} = 1/2$  is negligible (the dashed and solid lines overlap almost completely). We note that, considering the expressions for  $\Phi_{\Lambda, k|f, \gamma, n, \eta}(s)$  in Table III with  $S_1(s; \cdot)$  and  $S_2(s; \cdot)$  given in (28) and (29)

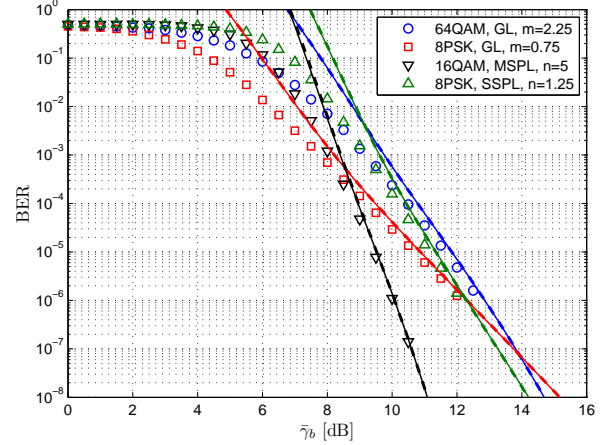


Fig. 4. BER of BICM transmission over fading AWGN channels for a 64-state convolutional code of rate 1/2. Nakagami- $m$  and Nakagami- $n$  fading with different parameters  $m$  and  $n$ . Solid lines: BER union bound using the saddlepoint approximation,  $\hat{s} = 1/2$  is assumed. Dashed lines: BER union bound using saddlepoint approximation, saddlepoint has been found numerically. (Note that solid and dashed lines overlap almost perfectly.) Markers are simulation results.

using the exponential approximations of the error function (50), we have provided tight BER approximations in terms of elementary functions.

4) *BER Results for Fading GMN Channels:* We now consider the case of both fading and GMN, and present selected BER results for different fading parameters,  $\epsilon$ -mixture noise parameters, and BICM constellations and labeling rules. Figure 5 compares the BER curves obtained from the BER union bound using the saddlepoint approximation (lines) and simulations (markers). For the saddlepoint approximation three cases are included: (i) the exact saddlepoint  $\hat{s}$  is determined for each SNR (solid lines), (ii) the asymptotic saddlepoint is determined from (42) and used for all SNRs (dashed lines), and (iii) the asymptotic saddlepoint approximation given in (44) is used (dash-dotted lines). Therefore the dash-dotted lines are obtained from a truly closed-form expression for approximating the BER. Also, solving (42) only once and over the small interval (43) requires little computational effort. The BER results confirm the usefulness of the proposed BER approximations for fading GMN. Clearly, the convergence of the union bound depends on the fading rate and mixture noise parameters. As can be seen from Figure 5, using asymptotic saddlepoint approximations gives relatively close union-bound approximations, with more noticeable gaps for the cases where the asymptotic analysis converges at lower BERs.

In Figure 6 the asymptotic BER results (lines) using the PEP expression (46) and only  $d_H = d_{\text{free}}$  are plotted together with the BER union bound (markers). In this figure, Nakagami- $m$ , Nakagami- $n$ , and Nakagami- $q$  fading distributions are used. For the evaluation of the asymptotic expressions the numerically found saddlepoint (solid lines) and the saddlepoint approximation  $\hat{s}_e$  from (44) (dashed lines) is applied. It can be seen that the asymptotic results correctly predict the diversity gain and the asymptotic coding gain of the BICM scheme. Furthermore, the closed-form saddlepoint approximation (44)

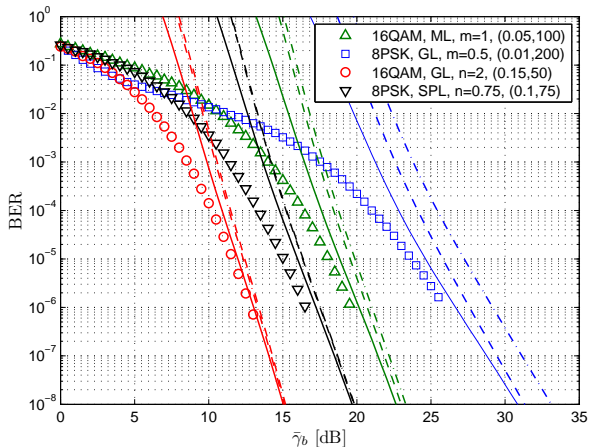


Fig. 5. BER of BICM transmission over fading channels impaired by  $\epsilon$ -mixture noise with parameters  $(\epsilon, \kappa)$  for a 64-state convolutional code of rate 1/2. Nakagami- $m$  and Nakagami- $n$  fading with different parameters  $m$  and  $n$ . Solid lines: BER union bound using saddlepoint approximation, saddlepoint has been found numerically. Dashed lines: BER union bound using saddlepoint approximation, the asymptotic saddlepoint from (42) is used. Dash-dotted lines: BER union bound using saddlepoint approximation, the asymptotic saddlepoint approximation given in (44) is used. Markers are simulation results.

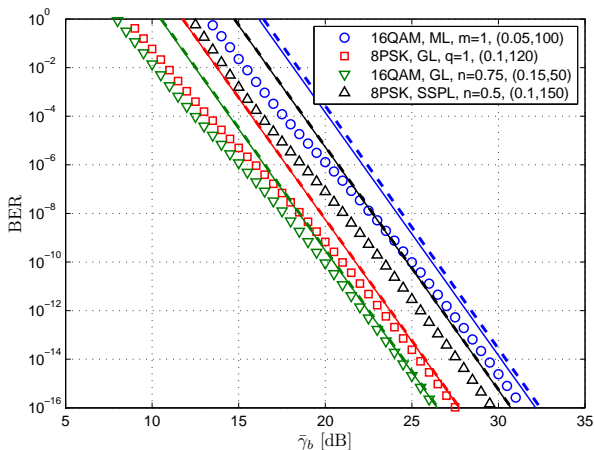


Fig. 6. BER of BICM transmission over fading channels impaired by  $\epsilon$ -mixture noise with parameters  $(\epsilon, \kappa)$  for a 64-state convolutional code of rate 1/2. Nakagami- $m$ , Nakagami- $n$ , and Nakagami- $q$  fading with different parameters  $m$ ,  $n$ , and  $q$ . Solid lines: Asymptotic BER from PEP (46) for  $d_H = d_{\text{free}}$  and numerically found saddlepoint. Dashed lines: Asymptotic BER from PEP (46) for  $d_H = d_{\text{free}}$  and the saddlepoint approximation  $\hat{s}_e$  from (44). Markers: BER union bound.

leads to negligible shifts in the asymptotic BER results. Hence, using (46) with  $\hat{s}_e$  from (44) allows us to approximate the asymptotic performance of BICM from a closed-form expression.

5) *Saddlepoint*: Finally, in Figure 7 we take a look at the evolution of the saddlepoint  $\hat{s}$  as function of the SNR  $\bar{\gamma}$  for the GMN cases studied in Figures 3 and 5. Also included are the asymptotic values for the saddlepoint (35) for nonfading and (42) for fading channels, and the asymptotic saddlepoint approximation (44) for fading channels, respectively. We observe that the saddlepoint strongly deviates from 1/2, the

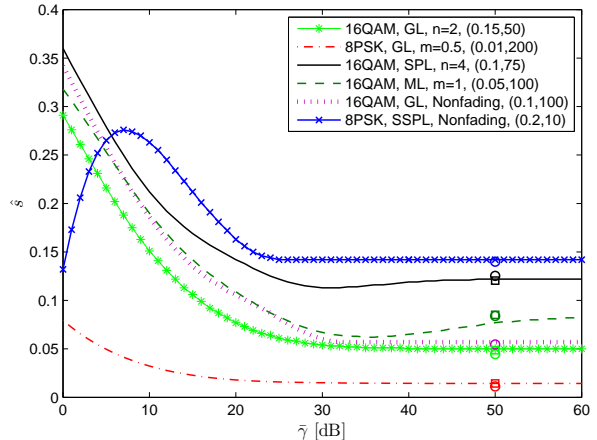


Fig. 7. Evolution of saddlepoint  $\hat{s}$  as a function of  $\bar{\gamma}$  for different constellations, labeling, and noise parameters. The circles indicate the asymptotic values of saddlepoint given in (35) for nonfading channels and in (44) for fading channels. The squares denote the exact asymptotic saddlepoint for fading channels given in (42).

solution for the AWGN case, and eventually converges to the value obtained through the asymptotic analysis developed in Section IV. The simple estimation given in (44) is shown to be reasonably accurate for these exemplarily cases. The range for  $\hat{s}$  strongly depends on the mapping rule, while its value at high SNR solely depends on the channel parameters as seen from (35) and (42).

## VI. CONCLUSIONS

BICM is a very popular spectrally and power efficient coded modulation scheme, whose BER analysis has received a lot of attention in the recent past. In this paper, we have extended and generalized previous approaches considering BICM transmission over general fading channels and additive GMN. We have derived closed-form approximations for the PDF of reliability metrics for the nonfading GMN channel, and its Laplace transform for fading GMN channels. Using the latter together with the saddlepoint approximation for PEP, we have provided a method for quick BER performance approximation. Since in the GMN case the saddlepoint needs to be computed numerically, we have also derived approximations for the (asymptotically) high SNR regime, which involve a single saddlepoint computation (for all SNR values) or are given in closed form. This analysis has also established expressions for the diversity and coding gain of BICM transmission over fading GMN channels. The presented numerical results have confirmed the relative accuracy of the analytical BER approximations for convolutionally coded BICM.

## REFERENCES

- [1] E. Zehavi, "8-PSK trellis codes for a Rayleigh channel," *IEEE Trans. Commun.*, vol. 40, no. 5, pp. 873–884, May 1992.
- [2] G. Caire, G. Taricco, and E. Biglieri, "Bit-interleaved coded modulation," *IEEE Trans. Inform. Theory*, vol. 44, no. 3, pp. 927–946, May 1998.
- [3] A. Guillén i Fàbregas, A. Martínez, and G. Caire, "Bit-interleaved coded modulation," *Foundations and Trends in Communications and Information Theory*, vol. 5, no. 1-2, pp. 1–153, 2008.

- [4] A. Martinez, A. Guillén i Fàbregas, and G. Caire, "Error probability analysis of bit-interleaved coded modulation," *IEEE Trans. Inform. Theory*, vol. 52, no. 1, pp. 262–271, Jan. 2006.
- [5] P.-C. Yeh, S. Zummo, and W. Stark, "Error probability of bit-interleaved coded modulation in wireless environments," *IEEE Trans. Veh. Technol.*, vol. 55, no. 2, pp. 722–728, March 2006.
- [6] L. Szczecinski, A. Alvarado, and R. Feick, "Distribution of max-log metrics for QAM-based BICM in fading channels," *IEEE Trans. Commun.*, vol. 57, no. 9, Sept. 2009.
- [7] A. Alvarado, L. Szczecinski, R. Feick, and L. Ahumada, "Distribution of L-values in Gray-mapped  $M^2$ -QAM: Closed-form approximations and applications," *IEEE Trans. Commun.*, vol. 57, no. 7, pp. 2071–2079, July 2009.
- [8] A. Martinez and A. Guillén i Fàbregas, "Large-SNR error probability analysis of BICM with uniform interleaving in fading channels," *IEEE Trans. Wireless Commun.*, vol. 8, no. 1, pp. 38–44, Jan. 2009.
- [9] A. Kenarsari-Anhari and L. Lampe, "An analytical approach for performance evaluation of BICM transmission over Nakagami-m fading channels," *IEEE Trans. Commun.*, 2010.
- [10] C. Goutis and G. Casella, "Explaining the saddlepoint approximation," *The American Statistician*, vol. 53, no. 3, pp. 216–224, Aug. 1999.
- [11] E. Biglieri, G. Caire, G. Taricco, and J. Ventura-Traveset, "Computing error probabilities over fading channels: A unified approach," *Eur. Trans. Telecommun.*, vol. 9, no. 1, pp. 15–25, Jan./Feb. 1998.
- [12] A. Martinez, A. Guillén i Fàbregas, and G. Caire, "New simple evaluation of the error probability of bit-interleaved coded modulation using the saddlepoint approximation," in *International Symposium on Information Theory and Applications (ISITA)*, Parma, Italy, Oct. 2004.
- [13] T. Li, W. Mow, and M. Siu, "Bit-interleaved coded modulation in the presence of unknown impulsive noise," in *IEEE International Conference on Communications (ICC)*, Istanbul, Turkey, June 2006, pp. 3014 – 3019.
- [14] A. Nasri and R. Schober, "Performance of BICM-SC and BICM-OFDM systems with diversity reception in non-Gaussian noise and interference," *IEEE Trans. Commun.*, vol. 57, no. 11, pp. 3316–3327, Nov. 2009.
- [15] D. Middleton, "Statistical-physical models of man-made radio noise-parts I and II," *U.S. Dept. Commerce Office Telecommun.*, April 1974 and 1976.
- [16] D. Stein, "Detection of Random Signals in Gaussian Mixture Noise," *IEEE Trans. Inform. Theory*, vol. 41, no. 6, pp. 1788–1801, Nov. 1995.
- [17] X. Wang and V. Poor, "Robust Multiuser Detection in Non-Gaussian Channels," *IEEE Trans. Signal Processing*, vol. 47, no. 2, pp. 289–305, Feb. 1999.
- [18] J.-W. Moon, T. Wong, and J. Shea, "Pilot-assisted and Blind Joint Data Detection and Channel Estimation in Partial-time Jamming," *IEEE Trans. Commun.*, vol. 54, no. 11, pp. 2092–2102, Nov. 2006.
- [19] M. Flury and J.-Y. Le Boudec, "Interference Mitigation by Statistical Interference Modeling in an Impulse Radio UWB Receiver," in *IEEE Intl. Conf. on Ultra-Wideband (ICUWB)*, Waltham, MA, Sept. 2006, pp. 393–398.
- [20] M. Zimmermann and K. Dostert, "Analysis and Modeling of Impulsive Noise in Broadband Powerline Communications," *IEEE Trans. Electromagn. Compat.*, vol. 44, no. 1, pp. 249–258, Feb. 2002.
- [21] J. Häring and A. Vinck, "Performance Bounds for Optimum and Suboptimum Reception under Class-A Impulsive Noise," *IEEE Trans. Commun.*, vol. 50, no. 7, pp. 1130–1136, July 2002.
- [22] A. Lapidoth and P. Narayan, "Reliable communication under channel uncertainty," *IEEE Trans. Inform. Theory*, vol. 44, no. 6, pp. 2148 – 2177, Oct. 1998.
- [23] A. Martinez, A. Guillén i Fàbregas, G. Caire, and F. Willems, "Bit-interleaved coded modulation revisited: A mismatched decoding perspective," *IEEE Trans. Inform. Theory*, vol. 55, no. 6, pp. 2756–2765, June 2009.
- [24] B. Classon, K. Blankenship, and V. Desai, "Channel coding for 4G systems with adaptive modulation and coding," *IEEE Trans. Wireless Commun.*, vol. 9, no. 2, pp. 8–13, April 2002.
- [25] A. J. Viterbi and J. K. Omura, *Principles of Digital Communication and Coding*. New York: McGraw-Hill, Inc., 1979.
- [26] W. Press, S. Teukolsky, W. Vetterling, and B. Flannery, *Numerical Recipes in C++*, 2nd ed. New York: Cambridge University Press, 2002.
- [27] C. Chan, "Combined Digital Phase and Amplitude Modulation Communication Systems," *IRE Trans. Commun. Systems*, vol. 8, pp. 150–155, Sept. 1960.
- [28] M. Chiani, D. Dardari, and M. Simon, "New exponential bounds and approximations for the computation of error probability in fading channels," *IEEE Trans. Wireless Commun.*, vol. 2, no. 4, pp. 840–845, July 2003.
- [29] M. K. Simon and M. S. Alouini, *Digital Communication Over Fading Channels*. New York: Wiley-Interscience, 2000.
- [30] Z. Wang and G. Giannakis, "A simple and general parameterization quantifying performance in fading channels," *IEEE Trans. Commun.*, vol. 51, no. 8, pp. 1389–1398, Aug. 2003.
- [31] A. Chindapol and J. Ritcey, "Design, analysis, and performance evaluation for BICM-ID with square QAM constellations in Rayleigh fading channels," *IEEE J. Select. Areas Commun.*, vol. 19, no. 5, pp. 944–957, May 2001.
- [32] X. Li, A. Chindapol, and J. Ritcey, "Bit-interleaved coded modulation with iterative decoding and 8PSK signaling," *IEEE Trans. Commun.*, vol. 50, no. 8, pp. 1250–1257, Aug 2002.



**Alireza Kenarsari-Anhari (S'09)** received his B.Sc. degree in electrical engineering from the University of Tehran, Tehran, Iran in 2007 and his M.A.Sc. degree in electrical and computer engineering from the University of British Columbia, Vancouver, BC, Canada in 2009. His main research interests are in communication theory. Currently, he is a software engineer at Dyaptive Systems, Vancouver, BC, Canada.



**Lutz Lampe (M'02, SM'08)** received the Diplom (Univ.) and the Ph.D. degrees in electrical engineering from the University of Erlangen, Germany, in 1998 and 2002, respectively. Since 2003 he has been with the Department of Electrical and Computer Engineering at the University of British Columbia, where he is currently an Associate Professor.

He is co-recipient of the Eurasp Signal Processing Journal Best Paper Award 2005 and the Best Paper Award at the 2006 IEEE International Conference on Ultra-Wideband (ICUWB). In 2003, he received the

Dissertation Award of the German Society of Information Techniques (ITG). He was awarded the UBC Killam Research Prize in 2008 and the Friedrich Wilhelm Bessel Research Award by the Alexander von Humboldt Foundation in 2009.

He is an Editor for the IEEE Transactions on Wireless Communications and the International Journal on Electronics and Communications (AEUE), and he has served as Associate Editor for the IEEE Transactions on Vehicular Technology from 2004 to 2008. He is Vice-Chair of the IEEE Communications Society Technical Committee on Power Line Communications. He was General Chair of the 2005 International Symposium on Power Line Communications and the 2009 IEEE International Conference on Ultra-Wideband.